Spatial properties of velocity structure functions in turbulent wake flows

E. Gaudin,[1] B. Protas,[1,2] S. Goujon-Durand,[1,3] J. Wojciechowski,[2] and J. E. Wesfreid[1]

[1]*Laboratoire de Physique et Mécanique des Milieux Hétérogènes, Centre National de Recherche Scientifique,*
Unité de Recherche Associée 857,
École Supérieure de Physique et Chimie Industrielles (ESPCI), 10 rue Vauquelin, 75231 Paris Cedex 05, France
[2]*Department of Aerodynamics, Institute of Aeronautics and Applied Mechanics,*
Warsaw University of Technology, Nowowiejska 24, 00-665 Warsaw, Poland
[3]*Faculté de Sciences et Technologie, Université Paris XII, Val de Marne 61, Avenue du Général de Gaulle,*
94010 Creteil Cedex, France

In this paper we present experimental evidence that the scaling laws for the velocity structure functions $S_n(r) = \langle [V(x+r) - V(x)]^n \rangle$ $n = 2,4,6,8$ hold in various parts of the flow domain. The exponents that characterize the scaling are, however, a function of the position in the wake that is the local strength and ubiquity of coherent structures. This variation is shown to be systematic and considerably exceeds the inaccuracy involved in the determination of the exponents. This is an objective indication of the influence that the organized flow structures and inhomogeneity may have on intermittency. In the analysis we invoke the concept of the extended self-similarity (ESS). [S1063-651X(98)50101-8]

PACS number(s): 47.27.Jv, 47.27.Nz, 47.27.Vf

One of the most intriguing features of fully developed turbulent flows is the phenomenon of intermittency [1]. It can be defined as significant departures from the mean exhibited by certain flow quantities [2]. In the analysis of intermittent aspects of turbulent flows attention is most often focused on the scaling properties of structure functions $S_n(r)$. The scaling $S_n \sim r^{\zeta_n}$ is usually examined, where ζ_n is the scaling exponent. Its deviation from the linear K41 prediction [3] may be regarded as a measure of the intermittency effects.

In recent years there appeared a lot of data, both experimental, e.g., Ref. [4], and numerical, e.g., Ref. [5], giving credit to the anomalous scaling of the structure functions. Besides, a number of theoretical models emerged, each of them attempting to predict the numerical values of the intermittency corrections. Recent works include Refs. [6–8]. All of them refer to the 3D homogeneous isotropic case and assume that the scaling exponents are uniquely defined and universal. In the turbulence research it has been customary to test the universality of the hypotheses against the variations of the Taylor scale Reynolds number Re_λ (e.g., Ref. [9]). On the other hand, in the present work we explore their dependence on the topological properties of the flow. Every laboratory experiment is contaminated by coherent structures. It is thus of great theoretical and practical interest to study how their presence affects the actual observed statistics of intermittency. An understanding of these effects may help to reinterpret the results obtained so far. Moreover, this can be regarded as a step towards reconciliation of the two apparently independent trends in turbulence research, namely analysis of the statistics and the study of coherent structures. An interesting attempt at such a combined analysis of turbulence of passive scalars was recently launched in Ref. [12].

Turbulent wake flows are characterized by a whole panoply of coherent structures [13] with varying degrees of intensity and regularity. Basic characteristics of these flows appear to be well documented in the literature [13–16]. Furthermore, wake flows can be relatively easily obtained in a laboratory. Therefore, this flow configuration appears particularly well suited to the analysis of inhomogeneous turbulence. Our work is the first systematic study of the scaling exponents in inhomogeneous turbulence.

In this work we show experimental evidence that the scaling laws of the structure functions exist in the various parts of the flow domain, although the values of the scaling exponents ζ_n in fact may be different. The ζ_n exponents presented below were obtained from hot-wire measurements performed in turbulent wake flows in two different experimental facilities (henceforth denoted as experiments $E1$ and $E2$). The parameters of the wind tunnel used in $E1$ are as follows: dimensions of the test section 20×20 cm, velocity range 0–12 m/sec, residual turbulence level 1.0%. In the case of the experiment $E2$ the respective parameters are: dimensions of the test section 30×30 cm, velocity range 0–50 m/sec, residual turbulence level 0.1%. In both cases, the thickness of the hot wire was 5 μm and its length 1.2 mm. The sampling frequency was 50 kHz, which gave the maximum resolution of a few Kolmogorov lengths η. The wake flow was generated by a circular cylinder with the diameter D equal to 1 cm. Data was recorded at a number of control points placed downstream from the obstacle on the axis of the flow (experiment $E1$) and both on and off the axis ($E2$). In the experiment $E1$ the downstream distances from the obstacle were 3, 5, 10, 30, 40, 60, and 80 D's. The overall number of control points in the experiment $E2$ exceeded 100. Their positions are shown in Fig. 1.

Each time series in the experiment $E1$ consisted of approximately 10^5 samples. In the experiment $E2$ the time se-
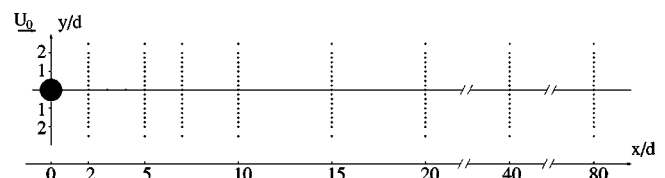
FIG. 1. Control points in the wake in the experiment $E2$.
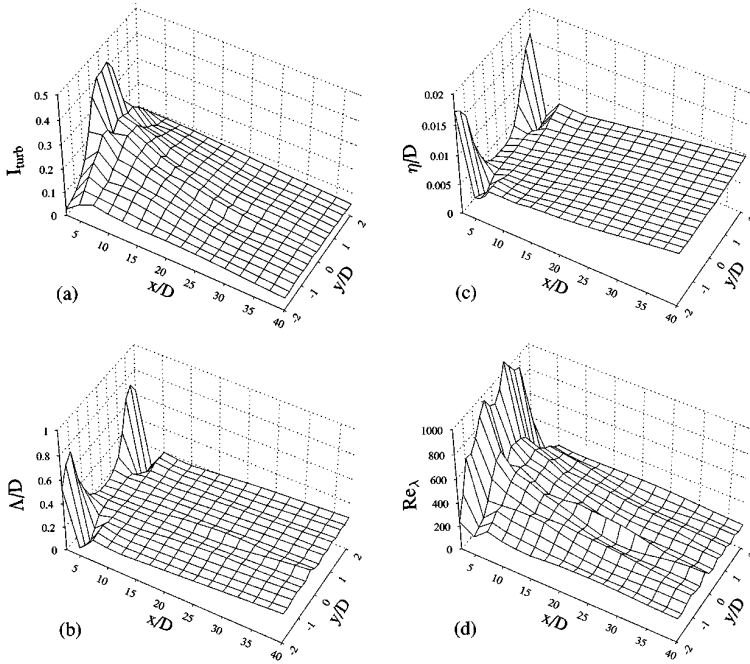
FIG. 2. Spatial evolution of turbulence intensity I_{turb} (top left), correlation length Λ (top right), dissipative scales η (bottom left) and the Taylor-scale-based Reynolds number Re_λ (bottom right). The mesh is interpolated using the nonuniformly spaced control points.

ries for the points on the axis were longer, around 5×10^5 samples each, and shorter for control points lying off the axis (between 10^3 and 10^4 each). Therefore convergence of higher (up to the 8th) order statistical moments of structure functions was assured for the former and only lower (up to the 4th) order for the latter locations [17]. For the sake of verification, at a few off-axis control points also longer time series (5×10^5) were acquired. Comparing to the shorter data, they showed no difference as concerns low-order statistics and other relevant flow quantities. In the following analysis the data from the experiment $E2$ will be mainly used. When the data from $E1$ appears, it will be explicitly stated. The *external* Reynolds number, i.e., based on the unperturbed flow velocity U_∞ and the obstacle diameter D, was around 6000 for the case $E1$ and 12 000 for the case $E2$. First we proceed with some standard diagnostics of the flow conditions. In Figs. 2(a)–2(d) we present the spatial behavior of some typical flow parameters: turbulence intensity I_{turb} ($I_{\text{turb}} = (u\text{rms}/u\text{mean}) \times 100\%$), correlation length Λ (see below for definition), Kolmogorov dissipation length η and Taylor scale based Reynolds number $\text{Re}_\lambda = (u_{\text{rms}}\lambda/\nu)$ (where $\lambda^2 = u_{\text{rms}}^2/\langle (du/dx)^2 \rangle$ is the Taylor microscale), respectively. Both Λ and η are nondimensionalized with respect to the cylinder diameter D. In all these figures the data in the nonuniformly spaced control points (Fig. 1) was interpolated in order to obtain a regular mesh. The plots are stretched in the spanwise direction. It is visible that the turbulence intensity I_{turb} and the Taylor scale based Reynolds number Re_λ have well defined maxima in the near vicinity of the obstacle and decay in the downstream and the spanwise directions. Conversely, both Λ and η remain approximately constant over the flow domain and increase only when the free stream is approached.

The dependence of the structure functions $S_n(r) = \langle |[V(x+r) - V(x)]|^n \rangle$ with $n = 2,3,4,6,8$ on the separation distance r normalized with respect to the Kolmogorov length η is shown in Figs. 3(a) and 3(b) for the downstream distances $x = 2D$ and $x = 80D$ along the axis, respectively.

The structure functions S_n are recovered from the time series by means of the standard Taylor hypothesis [18]. The scaling exponents are calculated using the technique of extended self-similarity (ESS), i.e., the structure function S_n is plotted against $S_3(r) = \langle |[V(x+r) - V(x)]|^3 \rangle$. The feasibility of this substitution was first established in Ref. [19] and is now commonly accepted. As was shown in Ref. [20], the specific form of the Taylor hypothesis does not affect the ESS scaling properties of the structure functions. Contrary to what was said in Ref. [10], ESS was also found to hold in the presence of shear, corresponding to the near wake region in
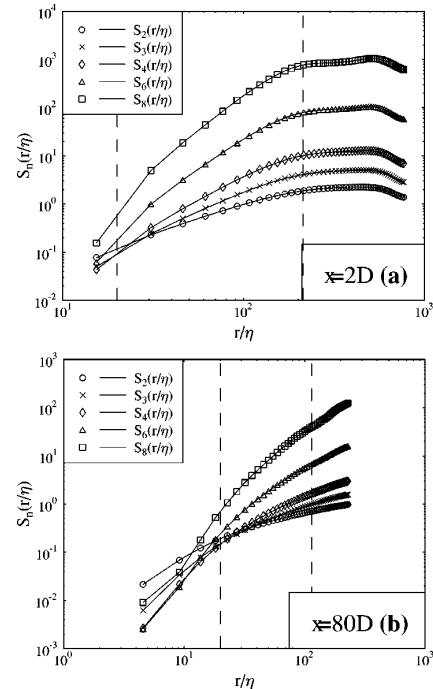
FIG. 3. Structure functions $S_n(r)$, $n = 2,3,4,6,8$ vs r/η at distances (a) $2D$ and (b) $80D$ downstream from the obstacle along the axis; the vertical dashed lines denote the limits of the ESS range.
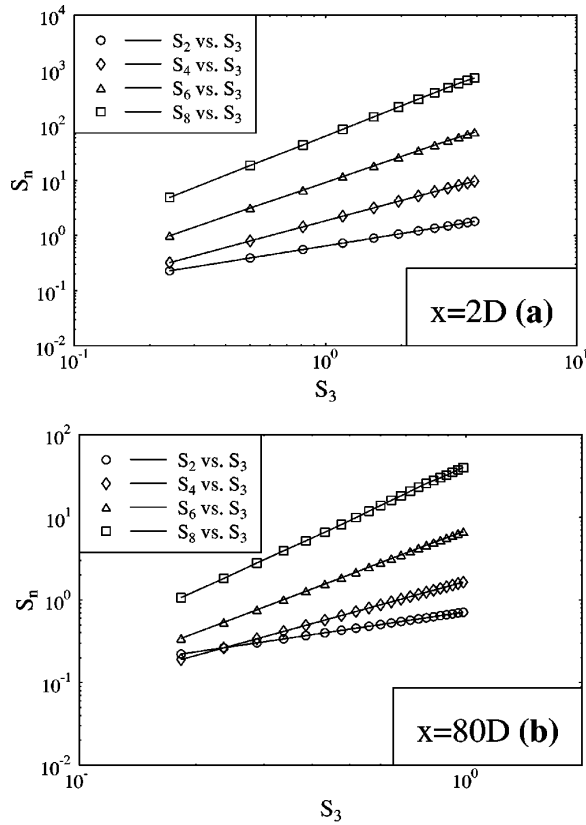
FIG. 4. ESS scaling of the structure functions $S_n(r)$, $n = 2,4,6,8$ at the distance: (a) $2D$ and (b) $80D$ downstream from the obstacle along the axis.

our case. In support of this statement, in Figs. 4(a) and 4(b) we present the ESS scaling of the structure functions of order $n = 2,4,6,8$ at the distances $2D$ and $80D$ downstream from the obstacle along the axis, respectively. It can be seen that in both cases the scaling is of comparable quality, although in the near wake region the ESS scaling range is slightly shorter, i.e., fewer pairs $\{S_n(r);S_3(r)\}$ can be taken into account in the evaluation of the scaling exponent. In Ref. [21] we also analyzed the variation of the characteristics of the ESS scaling range over the flow domain.

It was found in Ref. [22] that changes of the limits of the ESS range can influence the values of the scaling exponents. It was therefore necessary to introduce uniform criteria for the determination of the lower and upper bound of the scaling range. The lower limit was taken equal to a certain multiple of the Kolmogorov length η, usually around $(20–25)\eta$. This is in accordance with the values agreed upon in Ref. [23]. The upper limit corresponds to the lengths at which scaling ceases to be self-similar and is given in terms of the integral scale Λ defined as [24]

$$\Lambda = \frac{1}{b_{LL}(0)} \int_0^\infty b_{LL}(r)dr, \qquad (1)$$

where $b_{LL}(r)$ is the longitudinal correlation function for velocity:

$$b_{LL}(r) = \langle V(x+r)V(x) \rangle. \qquad (2)$$
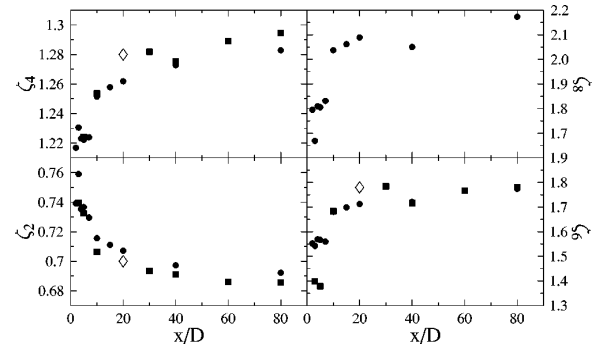
FIG. 5. Scaling exponents ζ_n, $n = 2,4,6,8$ on the axis of the wake as a function of the downstream distance from the obstacle. Circles correspond to the experiment $E2$, squares to the experiment $E1$, and diamonds to Ref. [19].

We assumed that the ESS range comprises scales up to around 0.5Λ. With the use of these criteria, it was possible to easily control the accuracy of the fit. As a result, the obtained error bars were small, considerably smaller than those reported in Ref. [19]. This is crucial as it shows that the discovered variations of the ζ_n exponents are generic and significantly exceed the uncertainties of their determination.

(a)

(b)
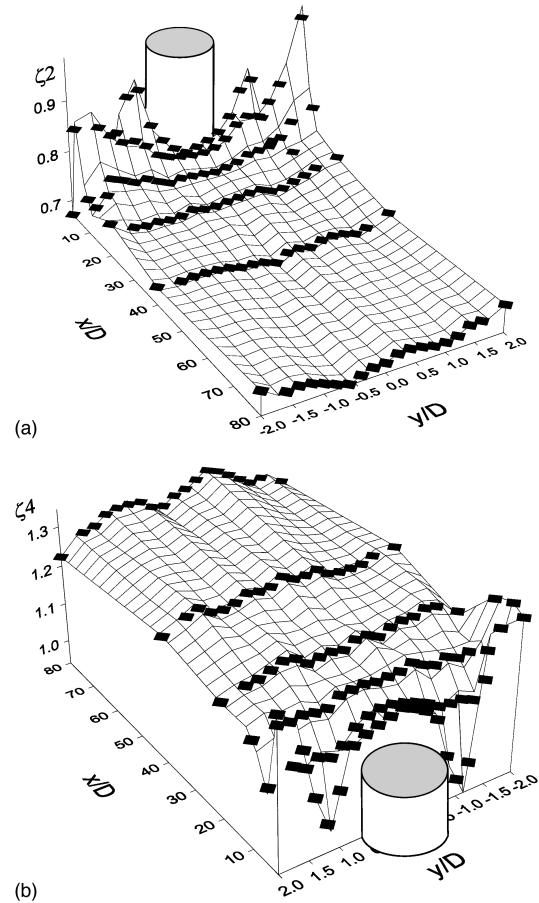
FIG. 6. 3D surface plots of the scaling exponents ζ_2 (a) and ζ_4 (b) as a function of the location in the wake. The solid symbol represents values actually obtained in the experiment $E2$. The surface meshes were computed using linear interpolation. Comparing to the actual proportions the plots are stretched in the spanwise direction. The cylindrical obstacle is also shown.

In Fig. 5 we present the exponents ζ_n, $n = 2,4,6,8$ as a function of the downstream distance from the obstacle. They correspond to the control points on the axis of the wake. The plots for $n = 2,4,6$ also include exponents obtained in the experiment $E1$ and reported in Ref. [19].

The consecutive Figs. 6(a) and 6(b) present the surface plots of the scaling exponents ζ_2 and ζ_4, i.e., their dependence on both the downstream distance from the obstacle and the spanwise separation from the axis of the wake. In these figures the solid symbols represent the values actually obtained in the experiment (on nonuniform grid–cf. Fig. 1), while the surface mesh was computed using linear interpolation. For the sake of clarity in the two figures different viewing perspectives have been taken and, comparing to the actual proportions, the plots are stretched in the spanwise direction. The figures also show the locations of the cylindrical obstacle.

The main result of the above graphs is that the values of the scaling exponents significantly depend on the location in the flow field where they are computed. This dependence seems to be systematic and exhibits well-defined trends. The intermittency correction, defined as the departure from the linear 1941 Kolmogorov (K41) prediction [1], is more pronounced in the near wake, especially off the axis, where it varies rapidly. On the other hand, in the far wake region the scaling exponents approach an asymptotic value that appears to be slightly more intermittent then the K41 prediction. In fact, it is close to the She and Leveque model [6]. The dependence of the scaling exponents ζ_n on the position in the flow domain indicates the role that the coherent structures and inhomogeneity play with regard to the intermittency correction. It shows the intrinsic relation between the small-scale statistics and the organized large-scale motion as well as flow topology. It must be added that we obtained similar results in a numerical simulation of the 2D turbulent wake flow [21] (where they were expressed in terms of the *relative* scaling exponents [27]). Influence of organized structures on the inertial range power laws was also found in the experiments reported in Ref. [26]. Actually, the exponents reported in Ref. [19] were also obtained in a wake, $x = 20D$ downstream from the cylinder. They agree remarkably well with our results computed at that particular location (cf. Fig. 5). This puts these, as well as other commonly accepted results, in a new perspective. This, in particular, concerns experiments performed in closed flows where coherent structures are more concentrated and the scaling exponents are indeed found to be more intermittent. In fact, these results are not in contradiction with certain theoretical models predicting the numerical values of the ζ_n exponents. For example, the She and Leveque model [6] includes one adjustable parameter that is the codimension of the most intermittent structures present in the flow. The nonuniformity of the ζ_n exponents may thus imply that the character of these structures may continually vary in the flow domain.

[1] U. Frisch, *Turbulence: the Legacy of A. N. Kolmogorov* (Cambridge University Press, Cambridge, 1995).

[2] C. M. Maneveau and K. R. Sreenivasan, J. Fluid Mech. **224**, 429 (1991).

[3] A. N. Kolmogorov, C. R. Acad. Sci. USSR **30**, 301 (1941).

[4] F. Anselmet, Y. Gagne, E. J. Hopfinger, and R. A. Antonia, J. Fluid Mech. **140**, 63 (1984).

[5] A. Vincent and M. Meneguzzi, J. Fluid Mech. **225**, 1 (1991).

[6] Z. S. She and E. Leveque, Phys. Rev. Lett. **72**, 336 (1994).

[7] Z. S. She and E. C. Waymire, Phys. Rev. Lett. **74**, 262 (1995).

[8] B. Dubrulle, Phys. Rev. Lett. **73**, 959 (1994).

[9] C. Baudet, S. Ciliberto, and P. Nhan Tien, J. Phys. II **3**, 293 (1993).

[10] R. Benzi, S. Ciliberto, C. Baudet, G. R. Chavarria, and R. Tripiccione, Europhys. Lett. **24**, 275 (1993).

[11] G. Karniadakis and G. Triantafyllou, J. Fluid Mech. **238**, 1 (1992).

[12] G. Stolovitzky, J. L. Aider, and J. E. Wesfreid, Phys. Rev. Lett. **78**, 4398 (1997).

[13] A. E. Perry and T. R. Stainer, J. Fluid Mech. **174**, 233 (1987); **174**, 271 (1987).

[14] D. K. Bisset, R. A. Antonia, and L. W. B. Browne, J. Fluid Mech. **218**, 439 (1990).

[15] H. C. Boisson, P. Chassaing, and H. Ha Minh, Phys. Fluids **26**(3), 653 (1983).

[16] D. A. Lyn, S. Einav, W. Rodi, and J.-H. Park, J. Fluid Mech. **304**, 285 (1995).

[17] Y. Gagne and E. Villermaux, in *Turbulence: A Tentative Dictionary*, edited by P. Tabeling and O. Cardoso (Plenum Press, New York, 1994).

[18] G. I. Taylor, Proc. R. Soc. London, Ser. A **164**, 476 (1928).

[19] R. Benzi, S. Ciliberto, C. Baudet, and G. R. Chavarria, Physica D **80**, 385 (1995).

[20] J.-F. Pinton and R. Labbe, J. Phys. II **4**, 1461 (1994).

[21] B. Protas, S. Goujon-Durand, and J. E. Wesfreid, Phys. Rev. E **55**, 4165 (1997).

[22] G. Stolovitzky and K. R. Sreenivasan, Phys. Rev. E **48**, R33 (1993).

[23] A. Arneodo *et al.*, Europhys. Lett. **43**, 411 (1996).

[24] A. S. Monin and A. M. Yaglom, *Statistical Fluid Mechanics* (MIT Press, Cambridge, MA, 1975), Vol. 2.

[25] H. Willaime, F. Belin, J. Maurer, and P. Tabeling, *Advances in Turbulence VI*, edited by S. Gavrilakis, L. Machiels, and P. A. Monkewitz (Kluwer, Dordrecht, 1996).

[26] F. Chilla, J.-F. Pinton, and R. Labbe, Europhys. Lett. **35**, 271 (1996).

[27] A. Babiano, B. Dubrulle, and P. Frick, Phys. Rev. E **52**, 3719 (1995).